LARGE EDDY SIMULATION OF A LIGHT GAS STRATIFICATION BREAK-UP BY AN ENTRAINING TURBULENT JET

Rüdiger Röhrig,[*] **Suad Jakirlić and Cameron Tropea**
Institute of Fluid Mechanics and Aerodynamics
Technical University of Darmstadt
Alarich-Weiss-Str. 10, 64287 Darmstadt, Germany
r.roehrig@sla.tu-darmstadt.de

ABSTRACT

The erosion process of a stratified light gas layer by a vertical turbulent jet of higher density inside a generic containment – investigated experimentally by Deri et al. (2010) – is studied computationally using Large Eddy Simulation (LES) as well as various RANS (Reynolds Averaged Navier-Stokes) models aiming at a comparative assessment of the different computational approaches for the considered case. With the methodology of LES included into the present model study, a novelty to date is established for jet-stratification-interaction inside generic containments. With respect to RANS, the high Reynolds models applied in the framework of this study include both the realizable k-ε Eddy Viscosity Model (EVM), see Shih et al. (1995), as well as the Reynolds Stress Model (RSM) as proposed by Gibson and Launder (1978).

INTRODUCTION

The specific configuration approached within this framework outlines a small-scale equivalent for the case of a hydrogen accumulation at elevated locations inside the containment of nuclear reactors resulting from a certain mode of failure such as the loss-of-coolant accident (LOCA). Presenting a considerably severe hazard due to the risk of hydrogen-oxygen-detonation, the goal is to erode the hydrogen stratification by means of a vertical air jet as motivated by the TH26 program of the Reactor Safety Research Project 150 1455, see Freitag et al. (2014). Since also experimental endeavours are made within this campaign, non explosion-prone helium is used as a substitute for hydrogen in the corresponding experiments and – for consistency – also within the computations. The particular containment configuration considered within the following is proposed by Deri et al. (2010), whose experimentally obtained data for the helium concentration over time at different vertical positions inside the containment are in turn exploited as reference fields. Prior to simulating the stratification break-up, the flow configuration of an axisymmetric turbulent jet is computed in order to validate the employed computational procedures and to approve the adopted mesh properties.

The eventual goal of the present investigation is to demonstrate LES' uprising capabilities for handling relevant engineering applications involving multi-species flows

with significant anisotropy and highly transient mixing processes, as they appear in e.g. gas turbine combustors, chemical processing plants, medical respiratory equipment or under floor air distribution systems. Additionally, the obtained LES results shall provide a database of the considered erosion process which allows for a term-by-term analysis and consequently further development of statistical turbulence models.

COMPUTATIONAL METHODOLOGY

By virtue of the fundamental principle of LES, the equations governing mass and momentum balance for the transient flow inside the containment are given by the filtered Navier-Stokes equations for variable-density Newtonian fluids as shown in Eq. (1) and (2), respectively.

$$\frac{\partial \bar{\rho}}{\partial t} + \frac{\partial (\bar{\rho} \widetilde{U}_i)}{\partial x_i} = 0 \tag{1}$$

$$\begin{aligned}
\frac{\partial (\bar{\rho} \widetilde{U}_i)}{\partial t} + \frac{\partial (\bar{\rho} \widetilde{U_j U_i})}{\partial x_j} &= -\frac{\partial \widetilde{p}}{\partial x_i} \\
+ \frac{\partial}{\partial x_j} &\left\{ \mu \left[\left(\frac{\partial \widetilde{U}_i}{\partial x_j} + \frac{\partial \widetilde{U}_j}{\partial x_i} \right) - \frac{2}{3} \delta_{ij} \frac{\partial \widetilde{U}_k}{\partial x_k} \right] \right\} + \bar{\rho} g_i
\end{aligned} \tag{2}$$

In the above expressions, the tilde-operator denotes a three-dimensional filter operation in space with a filter width of Δ, where the terms arising from commutation are not explicitly accounted for. The overlined density $\bar{\rho}$ represents the Favre-averaged density of the fluid and is calculated using the ideal gas law in combination with the mass fraction of the different species and their molar masses. The impact of gravity onto the fluid is considered by means of the body mass force g_i. Since the non-linear correlation $\widetilde{U_j U_i}$, as it appears in Eq. (2), is usually not known, the subgrid-scale (SGS) tensor $\tau_{ij} = \widetilde{U_i U_j} - \widetilde{U}_i \widetilde{U}_j$ is introduced, representing the part of the non-resolved motions in the governing equation for the resolved momentum, which needs to be modelled in order to close the equation. In this study, the well established approach according to *Boussinesq* is utilized, which assumes linearity between the SGS tensor τ_{ij}

---

[*]Corresponding author

and the filtered strain rate tensor $\widetilde{S}_{ij}$ according to

$$\tau_{ij} - \frac{1}{3}\delta_{ij}\tau_{kk} = -2\mu_t\left(\widetilde{S}_{ij} - \frac{1}{3}\delta_{ij}\widetilde{S}_{kk}\right). \qquad (3)$$

In Eq. (3), the artificial SGS viscosity μ_t is approximated according to the assumptions stated by Smagorinsky (1963) as

$$\mu_t = C_S\bar{\rho}\Delta^2|\widetilde{S}_{ij}|, \qquad (4)$$

where the model parameter C_S is dynamically evaluated as a function of the smallest resolved scales as suggested by Germano et al. (1991), whereas the least-square minimization according to Lilly (1991) is employed throughout this study in order to improve the stress-strain relationship. We refer to Fröhlich (2006) regarding implementation details for the dynamical Smagorinsky model.

Since the flow is of multi-component nature, a species transport equation governing the mass fraction of the two species is introduced according to

$$\frac{\partial(\bar{\rho}\tilde{c})}{\partial t} + \frac{\partial(\bar{\rho}\tilde{c}\widetilde{U}_i)}{\partial x_i} = \frac{\partial}{\partial x_i}\left(\mu\frac{\partial\tilde{c}}{\partial x_i} + \frac{\mu_t}{Sc_t}\frac{\partial\tilde{c}}{\partial x_i}\right), \quad (5)$$

where $\tilde{c} \in [0,1]$ denotes the filtered mass fraction of the light gas, i.e. helium for the present configuration. Eq. (5) is shown in its closed form, having applied the well established simple gradient diffusion model under use of the turbulent Schmidt number Sc_t. The molecular dynamic viscosity $\mu = f(x_i,t)$ of the binary gas mixture is calculated according to Mason and Saxena (1958) as a function of the individual viscosities and molar masses as well as the corresponding mass fraction. Since the configurations within the present frame are considered to be isothermal, the density of the flow is only a function of the species concentration and thus the use of the low Mach-number equations as introduced above is justified.

All computations were performed using OpenFOAM®, an open source computational fluid dynamics toolbox, utilizing a cell-centered finite volume method on an unstructured numerical grid. The solution procedure based on the implicit pressure algorithm with splitting of operators (PISO) for coupling pressure and velocity fields is employed within the time-accurate LES framework. The Large Eddy Simulation is performed using second-order accurate central differencing schemes for both convection and diffusion terms, whereas the temporal discretization follows a second-order implicit description. According to common practice, a maximum Courant number of $Co = 0.3$ is respected. The viscous sublayer of the near-wall regions is resolved, thus essentially resulting in a wall-resolved LES. With respect to the pipe section from which the air fountain emerges, the dimensionless grid spacings in azimuthal (Θ) and streamwise (z) directions are chosen to be in the order of $\Delta_\Theta^+ \approx 25$ and $\Delta_z^+ \approx 50$, respectively, while the first near-wall cell centers are located at $y^+ \approx 1$. The size of the computational domain spans over $46D \times 46D \times 65D$ and contains approximately one million cells, see Fig. 3.

NUMERICAL VALIDATION

In order to validate the employed LES procedure and to approve the adopted mesh properties, the case of a turbulent jet emerging from an axisymmetric pipe is computed prior to performing the erosion simulation. The bulk Reynolds number of the jet $Re_D = U_bD/\nu = 6800$ – with the diameter D, the bulk velocity U_b and the kinematic viscosity ν – is chosen to be identical to the one encountered during the subsequent helium erosion process, hence the fluid properties of air at ambient conditions are applied.

Fig. 1 shows the results for the mean streamwise velocity $\langle \widetilde{U}_z \rangle$ normalized by the corresponding centerline velocity U_{cl} as a function of the dimensionless radial coordinate $\eta = r/(z - z_0)$. Here, r represents the radial coordinate of the jet with its origin on the jet axis, whereas $z_0/D = -2.5$ is the virtual origin of the jet. The operator $\langle . \rangle$ denotes a temporal averaging operation over a sufficiently long interval. In addition to the streamwise velocity profile, the respective statistics of the mean velocity fluctuations in streamwise direction defined as $u_z \equiv \sqrt{\langle(\widetilde{U}_z - \langle\widetilde{U}_z\rangle)^2\rangle}$ are provided in Fig. 2.
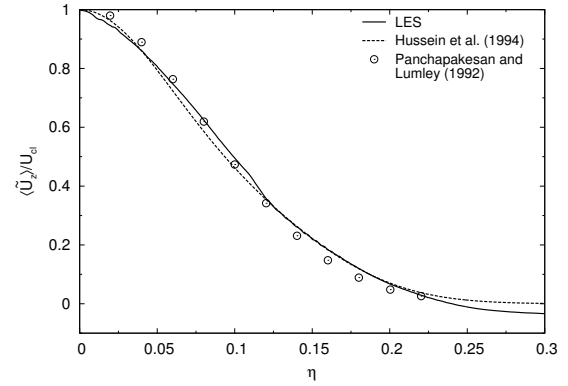

Figure 1: Normalized mean streamwise velocity as a function of the radial coordinate for the case of a turbulent axisymmetric jet at a bulk Reynolds number of $Re_D = 6800$. Results from the present LES evaluated at $z/D = 25$ are compared against experimental data as indicated in the corresponding legend.

The above comparisons against experimentally obtained data reveal a fair agreement for the performed LES and thereby confirm the applied numerical procedure as well as the chosen mesh dimensions. The deviations with increasing radial positions result from the fact that the turbulent jet was computed inside the confined geometry of the containment, thus essentially explaining the negative regime of $\langle\widetilde{U}_z\rangle$ for $\eta \geq 0.23$. To wrap up the non-dimensional description of the computed axisymmetric jet, the spreading rate $S = 0.094$ and the empirical constant $B = 5.8$ in $\langle\widetilde{U}_z\rangle/U_{cl} = B/(z/D - z_0/D)$ may be provided. These values are in reasonable agreement with experimentally obtained data, see e.g. Pope (2011).
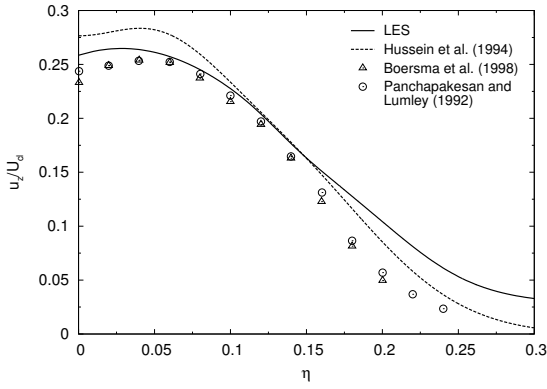
Figure 2: Normalized streamwise velocity intensity as a function of the radial coordinate for the case of a turbulent axisymmetric jet at a bulk Reynolds number of $Re_D = 6800$. Results from the present LES evaluated at $z/D = 25$ are compared against experimental and DNS data as indicated in the corresponding legend.

STRATIFICATION BREAK-UP: FLOW CONFIGURATION DESCRIPTION

The initial conditions of the flow configuration encountered in the following are given by a helium stratification in the upper vicinity of a cuboid containment with a height of $H = 1.29\,m$ and a square horizontal section of $B = 0.92\,m$, see Fig. 3. Apart from the helium layer, the containment is filled with air at ambient conditions thus resulting in a heterogeneous density distribution $\rho_m = f(z)$ along the vertical coordinate z of the configuration which is quantified in Fig. 4 for $t = 0\,s$.
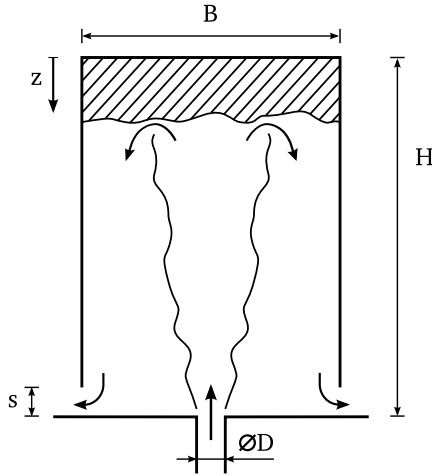

Figure 3: Schematic sketch of the present flow configuration: a helium stratification (shaded) inside a cuboid containment is eroded by means of an entraining turbulent air jet emerging from a pipe in the bottom plate.

The built-up layer of helium is then eroded over a period of $300\,s$ by means of an entraining turbulent round air jet which is fed into the containment through the bottom plate and is placed on the mid axis of the configuration. This

air fountain is successively penetrating the helium stratification and thereby transporting helium-rich fluid out of the configuration via a gap between the cuboid walls and the bottom plate with a height of s, see Fig. 3.

As indicated above, the bulk Reynolds number of the fountain is chosen to be $Re_D = 6800$ in order to match the experimental conditions encountered, in turn resulting in a local Froude number in the order of $Fr \sim \mathscr{O}(2)$. The definition of the local Froude number is here taken as $Fr = U_*/\sqrt{r_* \Delta_*}$, where U_* and r_* represent characteristic velocity and length scales at the interaction height and are assumed from the scaling laws of the undisturbed turbulent jet. The reduced gravity is accordingly given by $\Delta_* = g(\rho_j - \rho_m)/\rho_j$, where ρ_j and ρ_m are the densities of the turbulent air jet and the gas mixture inside the containment, respectively. Both species are taken at ambient conditions throughout the entire simulation duration.

To account for statistically steady, turbulent inlet conditions for the injected air fountain, a simultaneously performed precursor computation is employed which has a driving pressure gradient imposed to the momentum balance in order to maintain a constant mass flow rate corresponding to the respective flow Reynolds number. While the large eddy computation is performed on the full-scale domain, the unsteady RANS computations utilize symmetry conditions at both mid planes, thus essentially only accounting for one quarter of the experimental configuration.
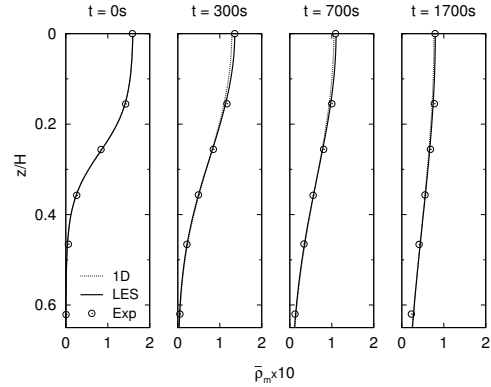

Figure 4: Evolution of the normalized density profile $\bar{\rho}_m = f(z, t)$ at different times for the case of pure diffusion, i.e. without air injection; experimental data from Deri et al. (2010).

In order to validate the behaviour of the numerical procedure for the case without feeding any air into the containment, i.e. for pure diffusion only, the temporal evolution of the initial stratification due to the presence of the vertical density gradient is computed and compared to experimentally obtained data. In addition to the full-scale coupled simulation, a one-dimensional numerical computation for the initial-boundary value problem of the species governing equation for zero velocity (see Eq. 5) is performed. The according solution is obtained using the piecewise non-linear Galerkin/Petrov-Galerkin method as proposed by Skeel and Berzins (1990) which is second-order accurate in space. Fig. 4 shows the resulting density profiles $\bar{\rho}_m = f(z, t)$ along the vertical axis for both approaches at different time

steps compared to the experimental data from Deri et al. (2010). The normalized mixture density is herein defined according to $\bar{\rho}_m = (\rho_j - \rho_m)/\rho_j$.

As the above comparison emphasizes, the plain diffusion process of the helium layer over time can be accurately captured using the present LES procedure. The additional match of the one-dimensional computation underlines the assumption that the diffusion process within the corresponding experiments is independent of the configuration geometry and confirms the correct functionality of the employed sensors.

In order to highlight the massive computational effort of approaching the present stratification erosion by means of LES, one may consider the simulation duration in terms of dimensionless time units $\tau = D/U_b$ which amounts up to $n_\tau = T/\tau = 76500$ for the period of air injection of $T = 300\,s$. With respect to contemporary computational resources, this effort corresponds to not less than $40 \cdot 10^3$ CPU hours on an Intel Xeon E5-2680 v3 architecture at a clock rate of $2.5\,GHz$.

STRATIFICATION BREAK-UP: RESULTS AND DISCUSSION

The experimental configuration considers four different phases during the performance of the layer erosion. At first, the helium layer is built up over a total duration of $300\,s$. This process, however, is not explicitly covered by the present computations. After $60\,s$ of rest, the air injection is engaged for a total of $300\,s$ and the resulting gas mixture is then monitored for the remaining time. The different phases of the experiment can e.g. be observed from Fig. 6a.

With the onset of the emerging turbulent fountain set to $t = 0$, the helium layer is gradually eroded by means of the penetrative behaviour of the impinging jet at the density interface[1], see Fig. 5. In order to monitor the entraining characteristics of the air fountain, Fig. 6 shows the temporal evolution of the binary gas mixture density $\bar{\rho}_m$ at different vertical positions for the computations using LES, RSM and EVM in comparison to experimental data. The lateral measurement position from which the shown data is extracted corresponds to the experimental one and is located next to the wall on an arbitrary symmetry plane of the domain. While the experimental data is averaged over a $0.1\,s$ window, no temporal averaging is used within the LES. The computational results, however, are spatially averaged by means of post-processing utilizing the two symmetry planes of the configuration.

The results obtained from the present LES are without any exceptions within an acceptable degree of conformity with respect to the experimentally obtained data. All local and global minima and maxima are captured correctly and apart from minor local deviations in the order of a few percent, the LES graphs coincide with the experimental results. Merely the peak around $t \approx 20\,s$ at $z/H = 0.36$ is not captured in its full extent. What might appear as a parasitic error from the measurements, is clearly an existing phenomenon. The numerical data unveil that the sudden temporary increase in concentration results from downwards flowing mixture from elevated positions which is eroded from the lower boundary of the stratification as soon as the fountain impinges on it. As the fountain continues to further
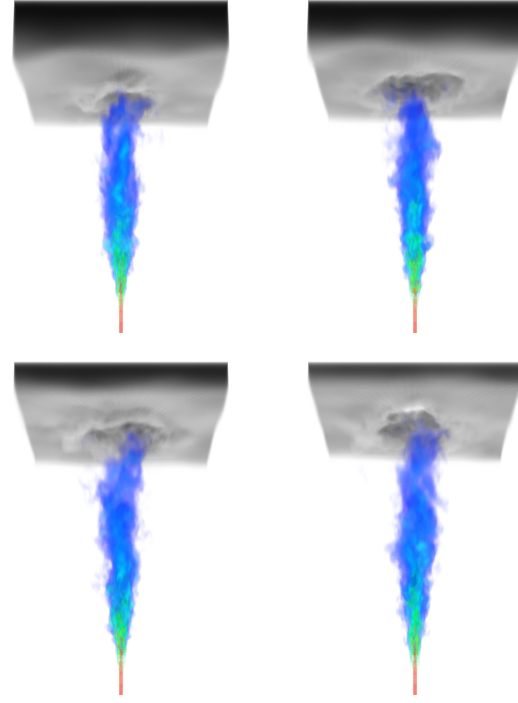
---

[1]Although the density distribution is essentially a smooth function, an interface between helium and air is approximately considered.

Figure 5: Exemplary illustration of the stratification break-up at $t = 22, 34, 71.5$ and $84\,s$ (from top left to bottom right). Helium concentration in gray scales, velocity magnitude in rainbow contours; color legends intentionally omitted for illustrative purposes.

penetrate the layer, the stratification stabilizes and the concentration is gradually increased rather than abrupt.

The experimental data reveal that the density profiles settle at a certain plateau once the air injection is stopped at $t = 300\,s$. Thus, the numerical computations are also put to an end once this stage is reached since the following diffusion process is of no interest for the dissolution of the remaining gas mixture.

For relevant stratification break-ups in practical applications, the quantity of major interest is commonly the rate at which the accumulated layer is dissolved below a certain threshold. In order to obtain a quantitative measure for the time until the layer is eroded, the half-life period t_{50} is introduced which marks the time where the instantaneous volume fraction drops below half of its initial value. The half-life period is used in its non-dimensional form $\tau_{50} = t_{50}/T$ in the following by means of normalization with the total duration of air injection T. From the previous definition, the desired erosion velocity $u_e = \partial z/\partial t_{50}$ is derived and transferred to its non-dimensional notation according to $\bar{u}_e = u_e/U_b$. The corresponding half-life periods of the helium layer are accordingly shown in Fig. 7 for the different computational approaches as well as a first order approximation extracted from the experimental data as obtained by Deri et al. (2010). While the LES provides a decent prediction of the half-life period and hence the erosion velocity, the RANS approaches yield considerable deviations from the experimental data. This behaviour, however, is consistent with literature if the simple gradient diffusion hypothesis is applied, see e.g. Zirkel (2011).

(a) $z/\mathrm{H} = 0$

(b) $z/\mathrm{H} = 0.16$

(c) $z/\mathrm{H} = 0.26$

(d) $z/\mathrm{H} = 0.36$

(e) $z/\mathrm{H} = 0.47$
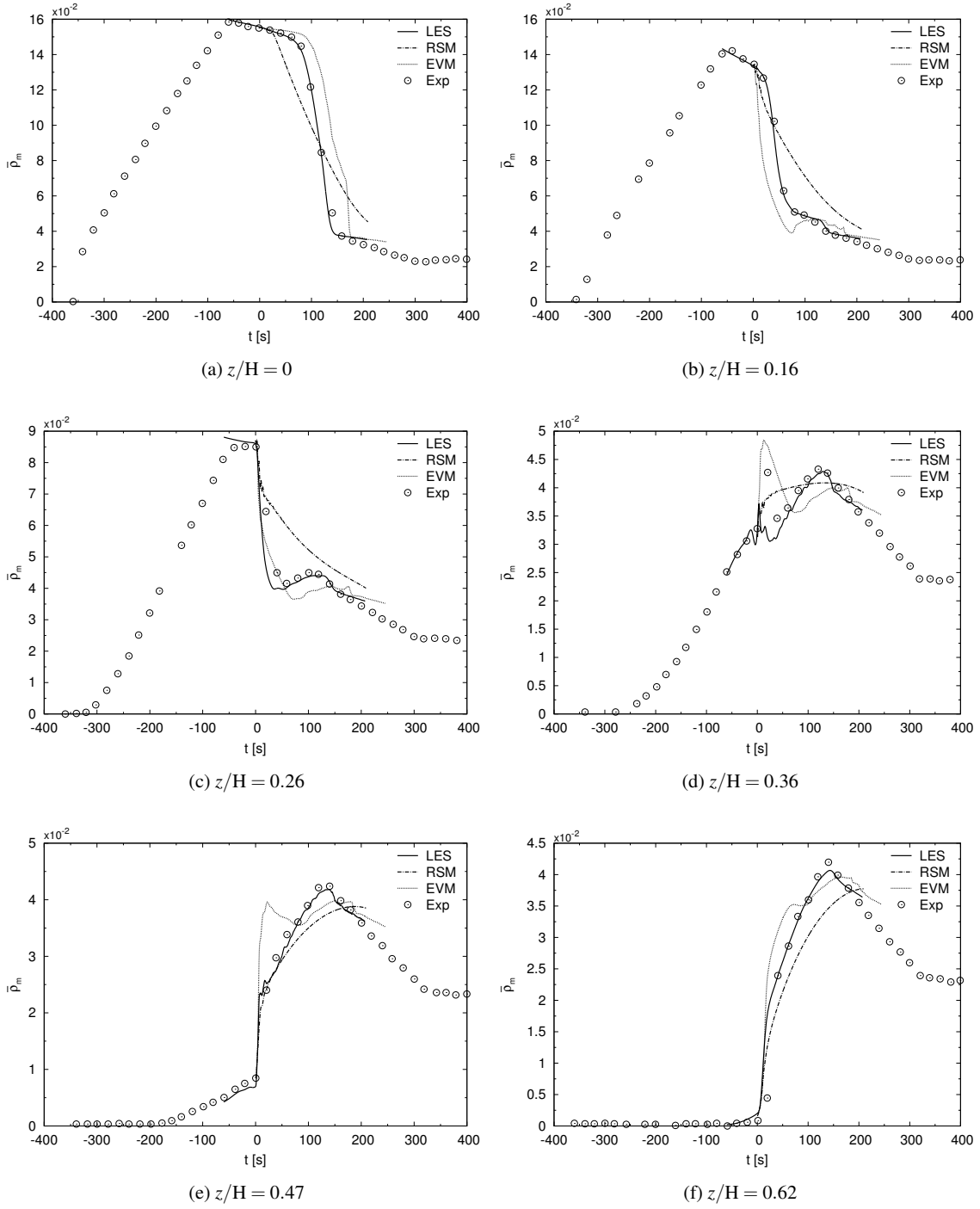
(f) $z/\mathrm{H} = 0.62$

Figure 6: Temporal evolution of the normalized mixture density $\bar{\rho}_m$ at various fixed positions z/H inside the containment. Experimental data taken from Deri et al. (2010) are compared against results obtained from LES, RSM and EVM computations.

From Fig. 7 a linearized approximation of the erosion velocity of $\bar{u}_e \approx 5.1 \cdot 10^{-4}$ is obtained. According to Lin and Linden (2005), the penetrative volume flux Q_p for a jet-stratification-interaction can be estimated as a function of the fountain volume flux Q_j following

$$Q_p = \frac{g_1'}{g_2' - g_1'} Q_j, \qquad (6)$$

where the reduced gravities g_1' and g_2' are defined according to $g_1' = g(\rho_1 - \rho_j)/\rho_j$ and $g_2' = g(\rho_2 - \rho_j)/\rho_j$. For the latter formulation, the inhomogeneous stratification is approximated to a lower layer with linear density variation and an upper layer of constant density. Thus, ρ_1 is assumed to equal the mean value of the lower layer while ρ_2 corresponds to the density within the homogeneous upper layer. With these assumptions stated, the erosion velocity according to Lin and Linden (2005) can be estimated from the ratio between the penetrative volume flux Q_p and the base area
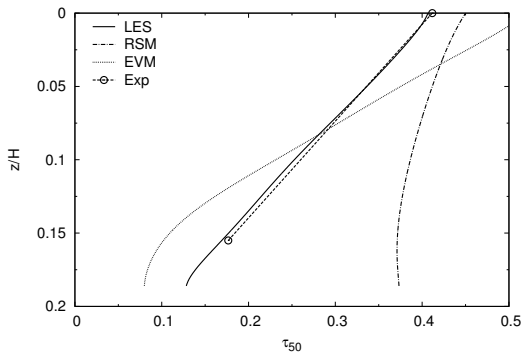
5

Figure 7: Evaluation of the normalized half-life period τ_{50} of the initial helium stratification. Experimental data taken from Deri et al. (2010) are compared against results obtained from LES, RSM and EVM computations.

of the containment, amounting to $\bar{u}_e \approx 4.2 \cdot 10^{-4}$. Thus, the estimation provides a decent prediction of the erosion velocity, bearing in mind that rather subjective assumptions and global flow properties were taken into account.

CONCLUSIONS

The present study embodies a highly transient, multi-species LES of the erosion process of a helium stratification by an entraining turbulent air jet inside a generic containment. The simulation results are compared against experimentally obtained data and evaluated regarding the overall penetrative behaviour of the eroding fountain. While the Large Eddy Simulation yields a decent prediction of the characteristic erosion process, the RANS approaches manage to capture the overall behaviour – though with a substantial lack in accuracy. The prediction of the entrainment rate using the theoretical approach as introduced by Lin and Linden (2005) is studied regarding its applicability for the considered case and essentially approved within limits. Despite the lack of detailed flow information in the vicinity of the interaction region between fountain and stratification prior to performing the computations, the methodology of Large Eddy Simulation is capable of reproducing the experimentally observed phenomena. This fact, is turn, may motivate to consider carefully achieved LES results as a frame of reference for configurations where experiments or direct numerical simulations are beyond the bounds of feasibility.

As a concluding remark it may be stated that due to the excessive duration of the experimental reference case in terms of physical time space, parts of the simulations are still element of ongoing work and will be reviewed during the conference talk.

REFERENCES

Boersma, B.J., Brethouwer, G. and Nieuwstadt, F.T.M. (1998), "A numerical investigation on the effect of the inflow conditions on the self-similar region of a round jet", Phys. Fluids, Vol. 10, pp. 899-909.

Deri, E., Cariteau, B. and Abdo, D. (2010), "Air fountains in the erosion of gaseous stratifications", Int. J. Heat Fluid Flow, Vol. 31, pp. 935-941.

Freitag, M., Gupta, S., von Laufenberg, B. and Schmidt-Naujok, E. (2014), "Technial Report TH26: Dissolution of a light gas stratification by air jet injection", Becker Technologies GmbH Eschborn, Technical Report 1501455.

Fröhlich, J. (2006), "Large Eddy Simulation turbulenter Strömungen", Teubner Verlag.

Germano, M., Piomelli, U., Moin, P. and Cabot W.H. (1991), "A dynamic subgridscale eddy viscosity model", Phys. Fluids, Vol. 3, pp. 1760-1765.

Gibson, M.M. and Launder, B.E. (1978), "Ground effects on pressure fluctuations in the atmospheric boundary layer", J. Fluid Mech., Vol. 86, pp 491-511.

Hussein, J., Capp, S.P. and George, W.K. (1994), "Velocity measurements in a high-Reynolds-number, momentum-conserving, axisymmetric, turbulent jet", J. Fluid Mech., Vol. 258, pp 31-75.

Lilly, D.K. (1991), "A proposed modification of the Germano subgrid-scale close method", Phys. Fluids A 4, pp. 633-635.

Lin, Y.J.P. and Linden, P.F. (2005), "The entrainment due to a turbulent fountain at a density interface", J. Fluid. Mech., Vol. 542, pp. 25-52.

Mason, E.A. and Saxena, S.C. (1958), "Approximate Formula for the Thermal Conductivity of Gas Mixtures", Phys. Fluids 1, Vol. 361.

Panchapakesan, N.R. and Lumley, J.L. (1993), "Turbulence measurements in axisymmetric jets of air and helium. Part 1. Air jet.", J. Fluid Mech., Vol. 246, pp 197-223.

Pope, S.B. (2011), "Turbulent Flows", Cambridge University Press.

Shih, T.-H., Liou, W., Shabbir, A., Tang, Z. and Zhu, J. (1995), "A New k-ε Eddy Viscosity Model for High Reynolds Number Turbulent Flows", Computers and Fluids, Vol. 24, No. 3, pp. 227-238.

Skeel, R. D. and M. Berzins (1990), "A Method for the Spatial Discretization of Parabolic Equations in One Space Variable", SIAM Journal on Scientific and Statistical Computing, Vol. 11, pp.132.

Smagorinsky, J. (1963), "General Circulation experiments with the primitive equations I. The basic experiment", Mon. Weather Rev., Vol. 91, pp. 99-164.

Zirkel, A. (2011), "Numerical investigation of the turbulence mass transport during the mixing of a stable stratification with a free jet", Institut fr Kernenergetik und Energiesysteme Stuttgart, PhD-Thesis.